# An *LCL-LC* Filter for Grid-Connected Converter: Topology, Parameter, and Analysis

Fei Li, *Student Member, IEEE*, Xing Zhang, *Senior Member, IEEE*, Hong Zhu, Haoyuan Li, and Changzhou Yu, *Student Member, IEEE*

***Abstract*—In order to further cut down the cost of filter for grid-connected pulsewidth modulation (PWM) converter under the more and more stringent grid code, a new kind of high-order filter, named *LCL-LC* filter, is presented in this paper. The resonant frequency characteristics of the filter are analyzed, and a parameter design method on the base of the characteristics is also proposed in the paper. The proposed parameter design method can easily make full use of the existing research results about the traditional *LCL* filter parameter design. And then a parameter robustness analysis method based on four-dimensional graphics is proposed to analyze parameter robustness of the presented filter. Compared with the traditional one, the proposed analysis method can analyze the filter performance under variations of several parameters at a time without any iteration. The comparative analysis and discussion considering the *LCL* filter, the trap filter, and the *LCL-LC* filter, are presented and verified through the experiments on a 5 kW grid-connected converter prototype. Experiment results demonstrate the accuracy of theoretical analysis and prove that the presented filter has a better performance than two others.**

***Index Terms*—*LCL* filter, *LCL-LC* filter, parameter design, parameter robustness analysis, trap filter.**

## I. Introduction

With the development of renewable energy sources, the grid-connected pulsewidth modulation (PWM) converter has been widely adopted, and an output filter is often used to limit the current harmonics caused by PWM [1]–[6]. However, the grid codes have become more and more stringent. For a grid-connected converter system, the standards such as the IEEE 519-1992 [7] and the IEEE 1547-2008 [8] require that each current harmonic of higher than the 35th should be limited to less than 0.3% of the rated fundamental current. Meanwhile, due to the increasing price of copper, the inductor becomes more and more expensive. If using a traditional *L* or *LCL* filter [9], [10] to filter PWM current harmonics to meet the aforementioned requirements, the cost of filter will increase significantly. So, it is a serious challenge to design a filter, which can make current harmonics meet the grid code requirements with the lowest possible cost [11]–[14].

In order to achieve better PWM harmonics attenuation and reduce the filter cost, the literatures [15] and [16] apply the trap filter [17], which contains an *LC* series resonant circuit, to attenuate switching harmonics in a grid-connected converter by making the *LC* circuit resonant at switching frequency. The trap filter can attenuate the switching frequency current harmonics much better than the *LCL* filter, leading to a decrease in the total inductance and cost. Generally, the significant harmonics of the converter output current will occur at multiples of switching frequency. Hence, in order to minimize the overall cost of the filter, Bloemink and Green [18] proposed a multituned traps filter that used the multiple *LC* series resonant circuits to bypass the current harmonics at the multiples of switching frequencies.

The trap filter and multituned traps filter can be thought of a combination of *LC* series resonant circuit(s) and *L* filter. The resonant circuit only works at the specified frequency. At other frequencies, the filter works as an *L* filter. So, the harmonic attenuation rates of the above two filters in the high-frequency band are only –20 dB/decade. It means that the two types of filters have the disadvantage of low-high-frequency harmonics attenuation rate. Even the traditional *LCL* filter has a better performance than the two filters. Some questions pop up immediately. If an *LCL* filter combines with an *LC* resonant circuit to form a new filter, can the filter solve the above problems? If so, what's the characteristic of the filter? How to design its parameters?

Based on the aforementioned questions, this paper presents a high-order filter topology, named *LCL-LC* filter, which is a combination of an *LCL* filter and an *LC* series resonant circuit. The presented filter has the ability of bypassing switching current harmonics and −60 dB/decade harmonics attenuation rate in the high-frequency band. The *LCL-LC* filter retains advantage of both the trap filter and the *LCL* filter.

In this paper, the presented *LCL-LC* filter is modeled and analyzed. And then two resonant frequency characteristics are obtained. A parameter design method for presented filter is proposed based on the obtained characteristics. The proposed parameter design method decomposes the whole filter parameter design into a traditional *LCL* filter part and an *LC* series resonant circuit part. In the proposed parameter design method, an *LCL* filter is designed first and then the whole *LCL-LC* filter parameters are obtained by designing the *LC* series resonant circuit parameters on the base of the designed *LCL* filter parameters. The advantage of proposed method is that the method can easily make full use of the existing research results about the

Manuscript received July 13, 2014; revised September 17, 2014; accepted October 29, 2014. Date of publication November 5, 2014; date of current version April 15, 2015. This work was supported in part by the National Natural Science Foundation of China under Project 51277051 and in part by the Specialized Research Fund for the Doctoral Program of Higher Education under Project 20130111110026. This paper was presented in part at the IEEE Region 10 Conference, Xi'an, China, Oct. 22–25, 2013. Recommended for publication by Associate Editor J. Pomilio.

The authors are with the School of Electrical Engineering and Automation, Hefei University of Technology, Hefei 230009, China (e-mail: sandflylf@gmail.com; honglf@ustc.edu.cn; zhhfut@163.com; 1160969033@qq.com; ycz87@163.com).

Color versions of one or more of the figures in this paper are available online at http://ieeexplore.ieee.org.

Digital Object Identifier 10.1109/TPEL.2014.2367135

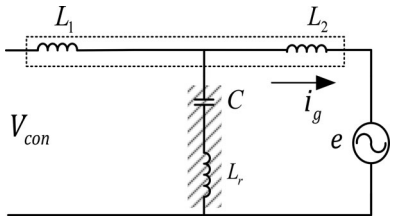


Fig. 1. Topology of the trap filter.

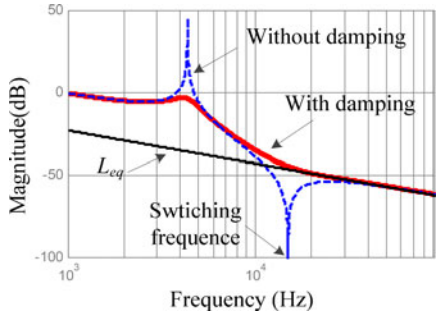


Fig. 2. Bode plots of trap filter and equivalent *L* filter.

traditional *LCL* filter parameter design. Meanwhile, as the parameter values may vary due to tolerance of filter components, working status or other reasons, it's necessary to analyze the robustness of parameters to check whether the current harmonics are still able to meet the grid code requirements under the variation. Traditionally, the bode plot and simulation are used to analyze the robustness of parameters. But they can only analyze one condition of parameter variation at a time. For the presented *LCL-LC* filter, the number of parameters is much bigger than the one of traditional *L* or *LCL* filter. The conditions of parameter variations are numerous when all combinations of different parameters are considered. It's very difficult to analyze the robustness of parameters in *LCL-LC* filter by traditional method in an acceptable time. In order to deal with this issue, a parameter robustness analysis method based on four-dimensional graphics is proposed. Compared with the traditional method, it can analyze that the conditions of several parameters variation at a time without iteration. In addition, it is very easy to find the weakest performance in all kinds of variations, which is very useful in parameter optimization.

This paper starts with an introduction of trap filter. Then the presented *LCL-LC* filter is described. The model and characteristics of filter are analyzed. Next, a parameter design method and a parameter robustness analysis method for the presented filter are proposed. Finally, the experiments of a 5 KW grid-connected converter are carried out to verify the theoretical analysis. And three kinds of filters—an *LCL* filter, a trap filter, and an *LCL-LC* filter—are compared.

## II. Principles of Trap Filter

Fig. 1 shows the topology of the trap filter which uses an *LC* series resonant circuit working at the switching frequency [15], [16]. The trap filter is composed of converter-side inductor $L_1$, grid-side inductor $L_2$, filter capacitor *C*, and resonant inductor $L_r$. Where $V_{\rm con}$ is the converter output voltage and $i_g$ is the grid current. The capacitor *C* and inductor $L_r$ compose a series resonant circuit, which resonates at the switching frequency to bypass the switching current harmonics. And the transfer function $i_g(s)/V_{\rm con}(s)$ of the trap filter can be derived as follows:

$$G_{\rm trap}(s) = \frac{L_r C s^2 + 1}{(L_1 L_2 C + (L_1 + L_2) L_r C) s^3 + (L_1 + L_2) s}. \tag{1}$$

The trap filter can be divided into two parts: a resonant circuit part (dashed area) and an inductor part (dotted box). Fig. 2 shows the bode plot of trap filter; it can be seen that the series resonant circuit can strongly attenuate the current harmonics around the switching frequency and lead to a decrease in the total inductance and cost.

The capacitor *C* can be thought of as open circuit in the frequency band lower than filter resonant frequency and the trap filter can be equivalent to as an *L* filter with $L_1 + L_2$ inductance. In the frequency band higher than series resonant frequency, the capacitor can be thought of as short circuit and the trap filter can be equivalent to an *L* filter with $L_{\rm eq}$ inductance, as shown in Fig. 2. Where the $L_{\rm eq}$ can be derived as

$$L_{\rm eq} = L_1 \left( \frac{L_2}{L_r} + 1 \right) + L_2. \tag{2}$$

From the earlier discussion, we can know that the trap filter can be equivalent to an *L* filter in the frequency band higher than the *LC* resonant frequency. So, in the high-frequency band, its harmonics attenuation rate is only $-20$ dB/decade. It means that grid-side current harmonic amplitudes at twice and more times of switching frequency may still be relatively high and cannot meet the requirements of grid codes.

There is a resonant peak in bode plot of trap filter. In order to damp it, a damping resistor is placed in the series resonant circuit. Fig. 2 also shows bode plots of a trap filter before and after damping resistor adding. It can be found that the resistor can effectively damp the resonant peak. However, it also weakens the ability of bypassing current harmonics and causes a great increase of harmonic amplitude at switching frequency.

## III. Presented *LCL-LC* Filter

### A. Topology and Modeling of the LCL-LC Filter

The trap filter can be considered as a combination of an *LC* series resonant circuit and an *L* filter. The series resonant circuit only works at the switching frequency. In the high-frequency band, the filter can be equivalent to an *L* filter. It is the reason why the harmonics attenuation rate in the high-frequency band is only $-20$ dB/decade.

Referring to the topology of trap filter, there is a conjecture that if an *LCL* filter combines with an *LC* resonant circuit to form a high-order filter, it may have both the ability of bypassing switching current harmonics and $-60$ dB/decade harmonics attenuation rate in the high-frequency band. Based on this idea, a high-order filter, named *LCL-LC* filter, is presented in this

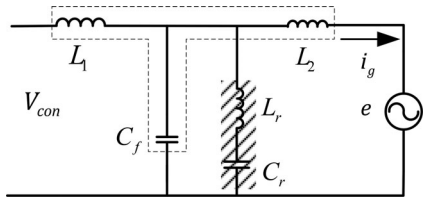


Fig. 3. Topology of *LCL-LC* filter.

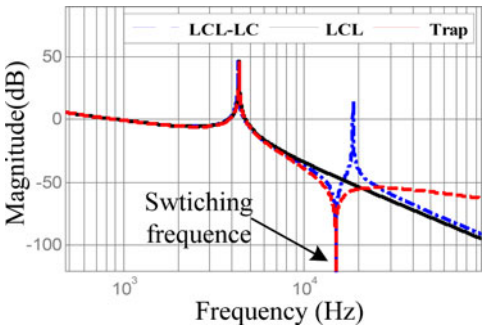


Fig. 4. Bode plots of *LCL* filter, trap filter, and presented *LCL-LC* filter.

paper. The topology of the filter, as shown in Fig. 3, is composed of a traditional *LCL* filter (dotted box) and a series resonant circuit (dashed area). The transfer function $i_g(s)/V_{\rm con}(s)$ of the presented filter can be derived as follows:

$$G_{LCL\text{-}LC}(s) = \frac{L_r C_r s^2 + 1}{As^5 + Bs^3 + Cs}. \tag{3}$$

Here, $L_1$ is the converter-side inductor, $L_2$ is the grid-side inductor, $C_f$ is the filter capacitor, $L_r$ is the resonant inductor, and $C_r$ is the resonant capacitor. And the parameters in the denominator are as follows:

$$\begin{aligned} A &= L_1 L_2 L_r C_r C_f \\ B &= L_1 L_2 (C_f + C_r) + L_r C_r (L_1 + L_2) \\ C &= L_1 + L_2. \end{aligned}$$

The *LC* circuit resonates at the switching frequency $\omega_{\rm sw}$

$$\omega_{\rm sw} = \frac{1}{\sqrt{L_r C_r}}. \tag{4}$$

Bode plots of three kinds of filters—*LCL* filter, trap filter, and presented *LCL-LC* filter—are shown in Fig. 4. From the figure, the following can be seen:

1) The bode plot of *LCL-LC* filter has a negative resonant peak at the switching frequency. It means the filter can effectively attenuate the switching frequency harmonics as the same as the trap filter.
2) The harmonic attenuation rate of an *LCL-LC* filter in high-frequency band is $-60$ dB/decade, which is the same as the one of an *LCL* filter.

The bode plots in Fig. 4 show that the presented filter has the advantages of both the trap filter and the *LCL* filter. And the conjecture at the beginning of this section is proved to be correct.

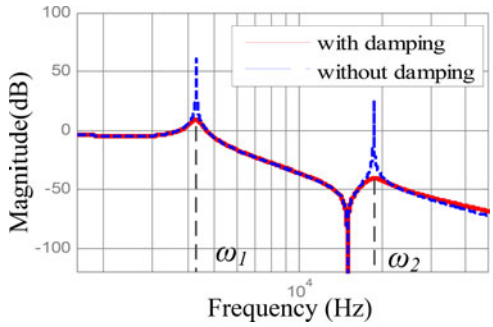


Fig. 5. Influence of damping resistor on the *LCL-LC* filter.

It can be seen from Fig. 5 that there are two resonant peaks in the bode plot of *LCL-LC* filter and the corresponding frequencies are noted as $\omega_1$ and $\omega_2$. The resonant peaks may cause system instability. In order to damp them, a damping resistor is placed in the branch of filter capacitor $C_f$. The damping resistor parameter design method and the power loss analysis were introduced in [19]–[23] in detail. Fig. 5 shows the bode plots of *LCL-LC* filter before and after addition of damping resistors. It can be found that the resistor can effectively damp the resonant peak and does not weaken the ability of bypassing current harmonics.

In summary, the presented filter combines the advantages of both the *LCL* filter and the trap filter and overcomes the shortcomings of the trap filter.

The similar topologies were reported in [18], [24]–[26]. However, they are different from the presented filter. The topology in [18] is a damping method of *LCL* filter, the *LC* circuit works at resonant frequency of *LCL* filter to reduce the peak gain at the resonant frequency of the filter. The topology in [24] is a damping method of *LLCL* filter. It applies the *RC* damping method [27], [28] used in an *LCL* filter to an *LLCL* filter. The method divides the capacitor *C* into two equal parts and places a damping resistor in one of the divided capacitors in order to reduce the power loss. Though the topologies of the filters mentioned earlier are similar to the presented filter, but the purpose and parameter design principles of them are different from the presented one. In [25] and [26], a high-order filter topology was proposed that contains more than one *LC* resonant circuit. It is very difficult to maintain the stability of converter system and design the filter parameters due to very high order and complex topology of the filter.

### *B. Resonant Frequency Characteristics*

In a grid-connected converter system, the resonant frequency of a filter is a very important parameter. There are two resonant frequencies in the *LCL-LC* filter. And the corresponding resonant frequency characteristics of the present filter are analyzed in this section [29].

From (3), the two resonant frequencies of the presented filter can be taken as follows:

$$\omega_1 = \sqrt{\frac{A + B - \sqrt{C + D + E}}{F}} \tag{5}$$

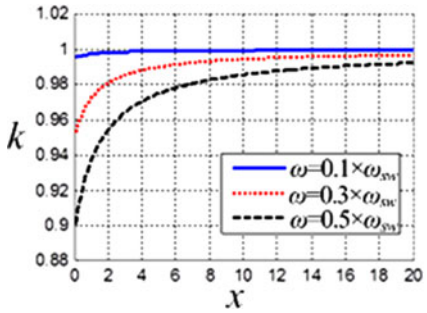


Fig. 6. Equation between factor $k$ and $x$.

$$\omega_2 = \sqrt{\frac{A + B + \sqrt{C + D + E}}{F}} \tag{6}$$

where

$$\begin{aligned} A &= L_1 L_2 (C_r + C_f) \\ B &= L_r C_r (L_1 + L_2) \\ C &= L_1^2 L_2^2 (C_r + C_f)^2 \\ D &= L_r^2 C_r^2 (L_1 + L_2)^2 \\ E &= 2 L_1 L_2 L_r C_r (L_1 + L_2)(C_r - C_f) \\ F &= 2 L_1 L_2 L_r C_r C_f . \end{aligned}$$

Suppose an *LCL* filter has the same capacitance and inductance as the ones of the *LCL-LC* filters. Namely, the value of converter-side inductor is $L_1$ and grid-side inductor is $L_2$. And the value of total filter capacitor is the same as the one of *LCL-LC* filter

$$C = C_r + C_f . \tag{7}$$

The resonant frequency of the *LCL* filter can be derived as follows:

$$\omega = \sqrt{\frac{L_1 + L_2}{L_1 L_2 C}} . \tag{8}$$

Assuming

$$x = \frac{C_f}{C_r} \tag{9}$$

$$k = \frac{\omega_1}{\omega} \tag{10}$$

$$c = \left(\frac{\omega}{\omega_{\mathrm{sw}}}\right)^2 . \tag{11}$$

Combining (5), (7)–(11), it can be derived as follows:

$$k = \sqrt{\frac{(c+1)(x+1) - \sqrt{(c+1)^2 (x+1)^2 - 4(x+1)c}}{2c}} . \tag{12}$$

Generally, in a grid-connected converter application, the range of $\omega$ is $0.1\ \omega_{\mathrm{sw}} < \omega < 0.5\ \omega_{\mathrm{sw}}$. According to (12), the equation between factor $k$ and $x$ is shown in Fig. 6. From Fig. 6, it can be seen that there is $1 > k > 0.9$. And in most cases, $x$ is greater than 1 and $\omega$ is less than $0.3\ \omega_{\mathrm{sw}}$. It can be found the value of $k$ is always greater than 0.97 under this condition. That means the value of $k$ is very close to 1. According to (10), we

TABLE I
SYSTEM PARAMETERS

| Rated Power: $P$ | Line Voltage: $E$ | DC Voltage: $U_{\mathrm{dc}}$ | Switching Frequency: $f_{\mathrm{sw}}$ |
|---|---|---|---|
| 5 kW | 110 Vrms | 200 V | 15 kHz |

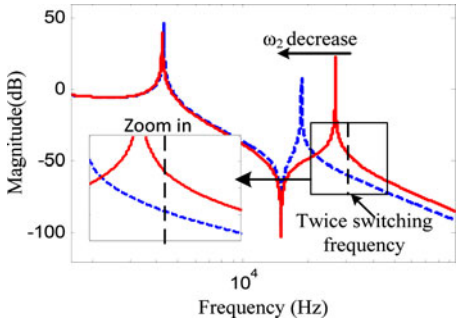


Fig. 7. Effect of second resonant frequency $\omega_2$ on the attenuation at the twice switching frequency.

TABLE II
DESIGNED FILTER PARAMETERS

| $L_1$ | $L_2$ | $C_f$ | $C_r$ | $L_r$ |
|---|---|---|---|---|
| 0.1 mH | 0.08 mH | 20 $\mu$F | 10 $\mu$F | 11 $\mu$H |

can get

$$\omega_1 \approx \omega . \tag{13}$$

That is to say, the resonant frequency of *LCL-LC* filter is similar to the one of *LCL* filter under the condition of the same capacitance and inductance. Fig. 4 shows the bode plots of three kinds of filters with the same capacitance and inductance. It can be found the resonant peaks of an *LCL* filter and an *LCL-LC* filter are overlapping.

In addition, from Fig. 4, it can be seen that bode plots of the two filter are almost the same within two-thirds of switching frequency. The presented filter has almost the same frequency response characteristic with traditional *LCL* filter. It means that the *LCL-LC* filter will not bring any extra control difficulties compared with *LCL* filter.

From the earlier analysis, the characteristic of the first resonant frequency in presented filter can be obtained. The second one will be illustrated as follows.

Assuming

$$k' = \left(\frac{\omega_2}{\omega}\right)^2 . \tag{14}$$

Combining (6)–(9), and (14), it can be derived as follows:

$$\left(\frac{\omega}{\omega_{\mathrm{sw}}}\right)^2 = \frac{(1 - k')(1 + x)}{k' + k' x - k'^2 x} . \tag{15}$$

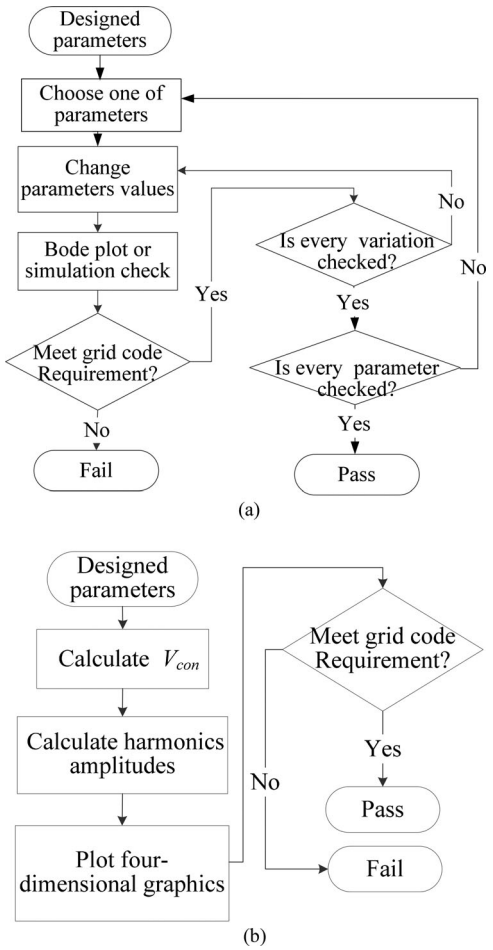


Fig. 8. Flowchart of parameter robustness analysis. (a) Traditional method. (b) Proposed method.

Assuming

$$k_1 = \left(\frac{\omega}{\omega_{\rm sw}}\right)^2 \approx \left(\frac{\omega_1}{\omega_{\rm sw}}\right)^2 \tag{16}$$

$$k_2 = \left(\frac{\omega_2}{\omega_{\rm sw}}\right)^2. \tag{17}$$

Taking (16) and (17) into (15), we can get

$$x = \frac{k_2 - k_1 + k_1 k_2}{k_2^2 - k_1 k_2 - k_2 + k_1}. \tag{18}$$

From (18), the second resonant frequency characteristic can be acquired that *x*, the ratio of filter capacitor $C_f$ and resonant capacitor $C_r$, can be obtained from the desired second resonant frequency $\omega_2$ when the $\omega_{\rm sw}$ and $\omega_1$ are certain.

## IV. Parameter Design

As mentioned before, the frequency response characteristic and the first resonant frequency of *LCL-LC* filter are similar to the ones of an *LCL* filter. As a result, a part of the presented filter parameters: converter-side inductor $L_1$, grid-side inductor $L_2$, and total capacitor *C* can be designed following the method

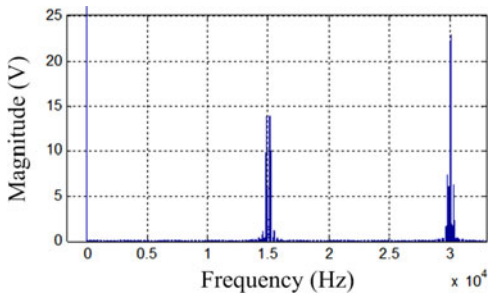


Fig. 9. Dominant PWM harmonic spectrum of converter output voltage.

TABLE III
Dominant PWM Voltage Harmonic of Converter

| Voltage harmonic | $V_{\rm con1}$ | $V_{\rm con2}$ | $V_{\rm con3}$ | $V_{\rm con4}$ |
|---|---|---|---|---|
| Magnitude (V) | 14 | 13.9 | 22.2 | 22.9 |
| Frequency (Hz) | 14 900 | 15 100 | 29 950 | 30 050 |

of traditional *LCL* filter parameter design. According to this, a parameter design method for an *LCL-LC* filter is proposed. The main idea of the proposed method is to decompose the whole presented filter parameter design into a traditional *LCL* filter part and an *LC* series resonant circuit part. The first part is to design the value of parameters: $L_1$, $L_2$, and *C* according to the method as the same as the one for a traditional *LCL* filter [30], [31], such as the control bandwidth, the limitation of current ripple and reactive power, and so on. The second part is to depart the total capacitance *C* into $C_f$ and $C_r$ according to the second resonant frequency characteristic and calculate the value of $L_r$ according to (4).

The following example of 5 KW grid-connected converter system illustrates a step-by-step procedure of proposed parameter design method. The parameters of converter system are listed in Table I.

### A. Design of the Converter-Side Inductor $L_1$

Assuming the modulation index m is 0.9 and allowable THD of converter-side inductor current is no more than 10%, the value of $L_1$ can be derived as follows [32]:

$$L_1 = \frac{1}{3\sqrt{2}} \frac{E^2}{100P} \frac{f_0}{f_{\rm sw}} \frac{1}{\rm THD} \sqrt{\frac{3}{2} - \frac{4\sqrt{3}m}{\pi} + \frac{9m^2}{8}} \approx 0.1\,{\rm mH}$$

where $f_0$ is the fundamental frequency.

### B. Design of Total Filter Capacitance *C*

The value of total filter capacitance *C* is designed to 30 $\mu$F to limit the reactive power to 2.5% of rated power

$$C = \frac{2.5\% \times P}{100\pi E^2} \approx 30\,\mu{\rm F}.$$

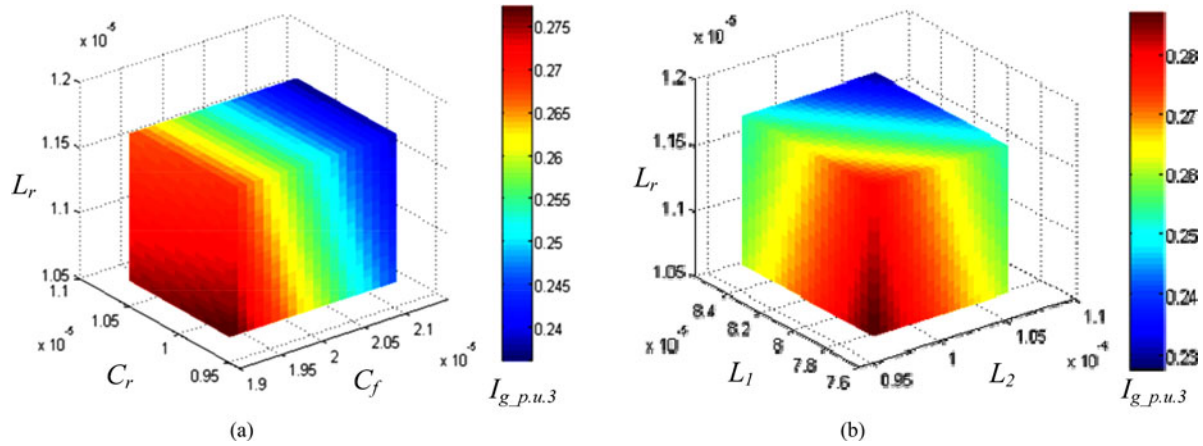


Fig. 10. Variation trend of $I_{\mathrm{g\,p.u.3}}$ while the filter parameters vary from 95% to 105% of designed value. (a) $L_r$, $C_r$ and $C_d$ variation. (b) $L_r$, $L_1$, and $L_2$ variation.

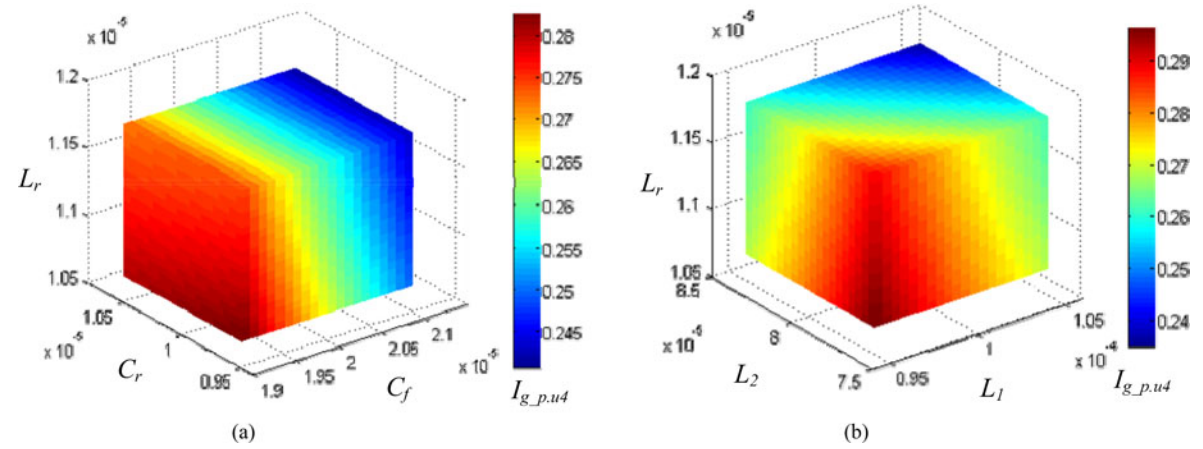


Fig. 11. Variation trend of $I_{\mathrm{g\,p.u.4}}$ while the filter parameters vary from 95% to 105% of designed value. (a) $L_r$, $C_r$, and $C_f$ variation. (b) $L_r$, $L_1$, and $L_2$ variation.

### C. Design of Grid-Side Inductor $L_2$

The first resonant frequency $\omega_1$ is set to be 28 000 rad/s (about 0.3 times $\omega_{\mathrm{sw}}$) according to the requirement of control bandwidth. From (8) and (13), the value of grid-side inductor $L_2$ can be taken as follows:

$$L_2 \approx \frac{L_1}{L_1 C \omega_1^2 - 1} \approx 0.08\,\mathrm{mH}.$$

### D. Design of Capacitor $C_r$ and $C_f$

From (18), it can be seen that if the $\omega_2$ is set, the factor $x$ can be calculated easily and then the value of $C_r$ and $C_f$ can be obtained according to (7) and (9).

To set the $\omega_2$, the following rules should be considered:

1) The smaller the second resonant frequency $\omega_2$ is, the greater the attenuation of the twice switching frequency harmonics is, as shown in Fig. 7.
2) The second resonant frequency $\omega_2$ should not be close to the switching frequency, in order to avoid the amplification of switching frequency harmonics. Besides, the values of parameters may vary due to components tolerance, working status or other reasons, the real value of $\omega_2$ will be different from the setting one and may close to the switching frequency which will also amplify the switching current harmonics seriously. So, the setting value of $\omega_2$ should keep a certain distance away from the switching frequency to make sure the real value of $\omega_2$ is different from the switching frequency under the all conditions of variation.

Considering the above rules, the value of $\omega_2$ is set to 11310 rad/s (18 kHz). The factors $k_1$ and $k_2$ can be taken as follows:

$$k_1 = \left(\frac{\omega_1}{\omega_{\mathrm{sw}}}\right)^2 = 0.09, \qquad k_2 = \left(\frac{\omega_2}{\omega_{\mathrm{sw}}}\right)^2 = 1.44.$$

Substituting them into (18)

$$x = \frac{k_2 - k_1 + k_2 k_1}{k_2^2 - k_2 k_1 - k_2 + k_1} = 2.49.$$

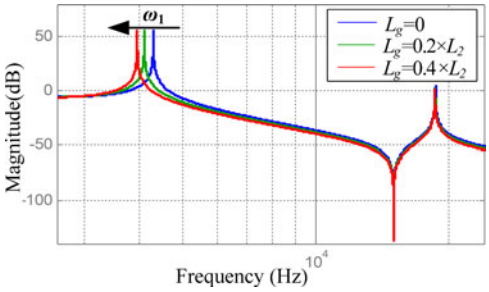


Fig. 12. Effect of weak grid condition on the filter resonant frequencies.

TABLE IV
VALUE OF THREE FILTERS PARAMETERS

| Parameter | *LCL* | *LLCL* | *LCL-LC* |
|---|---|---|---|
| $L_1$ | 0.1 mH | 0.1 mH | 0.1 mH |
| $L_2$ | 0.08 mH | 0.08 mH | 0.08 mH |
| $C\,(C_f)$ | 30 $\mu$F | 30 $\mu$F | 20 $\mu$F |
| $C_r$ | – | – | 10 $\mu$F |
| $L_r$ | – | 3.8 $\mu$H | 11 $\mu$H |

According to (7) and (9), the values of $C_r$ and $C_f$ can be taken as follows:

$$C_f = \frac{x}{1+x}C \approx 20\,\mu\text{F}$$
$$C_r = \frac{1}{1+x}C \approx 10\,\mu\text{F}.$$

### *E. Design of Resonant Inductor $L_r$*

The resonant inductor $L_r$ can be calculated as follows according to (4):

$$L_r = \frac{1}{C_r\omega_{\text{sw}}^2} \approx 11\,\mu\text{H}.$$

The designed *LCL-LC* filter parameters are listed in Table II.

According to (5), (6), and the parameters in Table II, the resonant frequency $\omega_1$ is designed to 27 018 rad/s (4.3 kHz) and $\omega_2$ is designed to 116 872 rad/s (18.6 kHz). The errors between them and set values are less than 4%, which can be ignored.

## V. PARAMETER ROBUSTNESS ANALYSIS

The value of filter parameters may vary due to components tolerance, working status, or other reasons. So, it's is very important to analyze the robustness of designed parameters to check whether the current harmonics are still able to meet the grid code requirements under all kinds of variations.

The bode plot and simulation are used to analyze parameter robustness of *LCL* filter [33], [34]. But they can only analyze one kind of variation at a time. A flowchart of a traditional parameter robustness analysis procedure is shown in Fig. 8(a). It can be found that lots of iteration should be done. Generally, only maximum variation of each parameter is checked in order to finish the analysis in an acceptable number of steps. But the variation trend of current harmonics with parameter variations can't be achieved in the traditional analysis method.

Compared with *L* or *LCL* filter, the number of parameters in presented *LCL-LC* filter is very big. The conditions of variation are numerous. It's very difficult to analyze parameter robustness of the presented *LCL-LC* filter by the traditional method.

In order to analyze parameter robustness of the presented filter, a parameter robustness analysis method based on four-dimensional graphics is proposed. And a flowchart of proposed parameter robustness analysis procedure is shown in Fig. 8(b). The proposed method calculates the amplitudes of dominant current harmonics under all kinds of parameter variations. And then the amplitudes are plotted with four-dimensional graphics which can distinctly show the maximal point of current harmonics and variation tendency. The detailed procedure of proposed parameter robustness analysis under the conditions of each parameter variation in 5% of designed value is shown as follows.

According to the filter topology in Fig. 3, the amplitude of filter grid-side current harmonics $I_{gp.u.}$ can be calculated as follows:

$$I_{g\_\text{p.u.}} = \frac{V_{\text{con}} \times |G_{LCL\text{-}LC}(\omega)|}{I_n} \times 100\% \tag{19}$$

where $I_n$ is the peak value of converter rated current and $|G_{LCL\text{-}LC}(\omega)|$ is the amplitude of the *LCL-LC* filter transfer function at frequency $\omega$. The $I_n$ can be taken as follows:

$$I_n = \frac{\sqrt{2}P}{\sqrt{3}E}. \tag{20}$$

The $V_{\text{con}}$ can be obtained by simulation or according to [35]. Fig. 9 shows the harmonic spectrum of $V_{\text{con}}$ under the condition that the modulation index m is 0.9. And the four dominant PWM harmonics amplitudes of converter output voltage $V_{\text{con}}$, noted as $V_{\text{con1}}$, $V_{\text{con2}}$, $V_{\text{con3}}$, and $V_{\text{con4}}$, and the corresponding frequencies are listed in Table III.

From Table III, it can be seen that the dominant harmonics of the converter output voltage occur at the frequencies of $f_s \pm 2f_0$ and $2f_s \pm f_0$. $V_{\text{con1}}$ and $V_{\text{con2}}$ are sideband voltage harmonics of the switching frequency and $V_{\text{con3}}$, $V_{\text{con4}}$ are the sideband voltage harmonics of the twice switching frequency.

The presented filter is a low-pass filter with an ability of bypassing switching frequency current harmonics. So, its dominant current harmonics occur around twice switching frequency. There are two dominant current harmonics. Taking $V_{\text{con3}}$, $V_{\text{con4}}$, and corresponding frequencies in Table III into (19), the amplitudes of dominant current harmonics $I_{gp.u.3}$ and $I_{gp.u.4}$, can be obtained. Then the four-dimensional graphics are used to show the variation trend of dominant current harmonics amplitudes. The colors in Fig. 10 show the variation trend of $I_{gp.u.3}$ while the filter parameters: $L_r$, $C_r$, and $C_f$ in Fig. 10(a) and $L_r$, $L_1$, and $L_2$ in Fig. 10(b) vary from 95% of designed value to 105% of designed value. The colors in Fig. 11 show variation trend of $I_{gp.u.4}$ while the filter parameters $L_r$, $C_r$, and $C_f$ in Fig. 11(a) and $L_r$, $L_1$, and $L_2$ in Fig. 11(b) vary from 95% of designed value to 105% of designed value. From Figs. 10 and 11, it can be found that the maximum of dominant current harmonics under all kinds of parameter variations is still less than 0.3%. So,

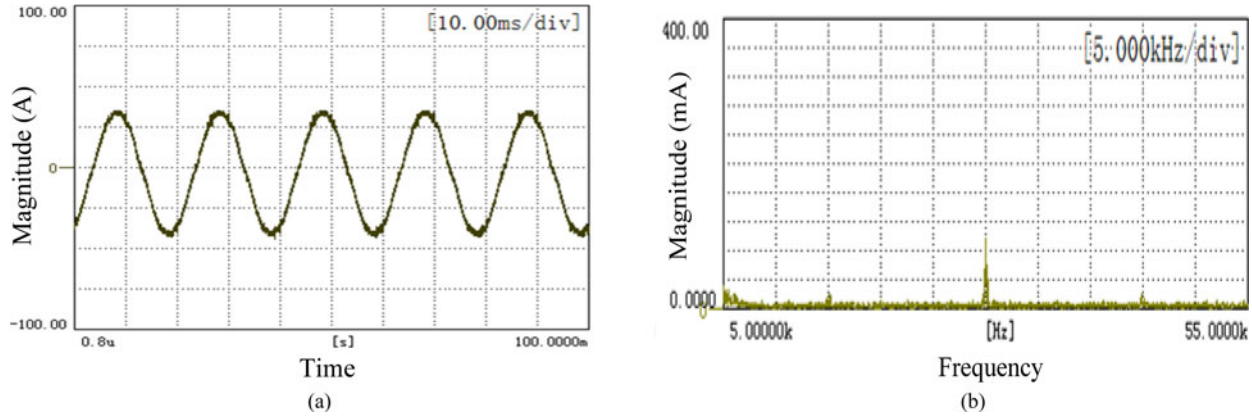


Fig. 13. Grid current waveform and corresponding FFT analysis result in *LCL-LC* filter. (a) Grid current waveform. (b) FFT analysis.

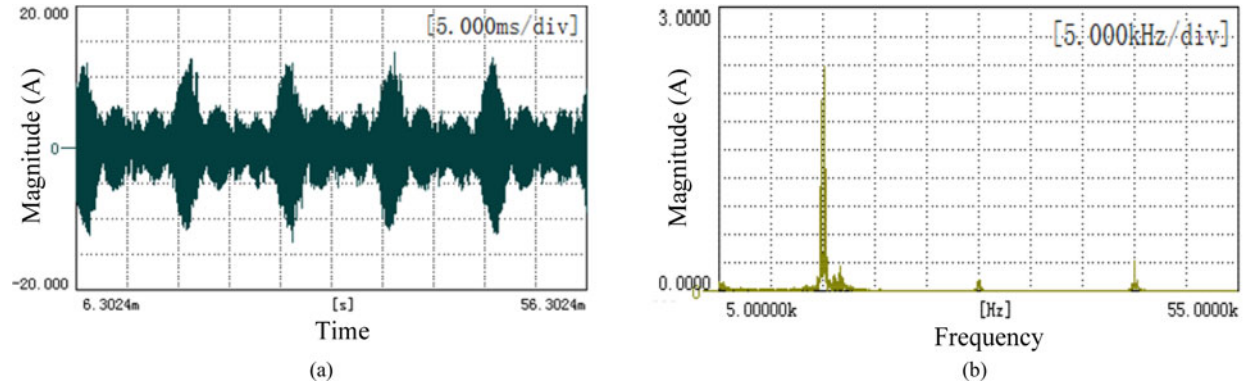


Fig. 14. Resonant circuit current waveform and corresponding FFT analysis result in *LCL-LC* filter. (a) Resonant circuit current waveform. (b) FFT analysis.

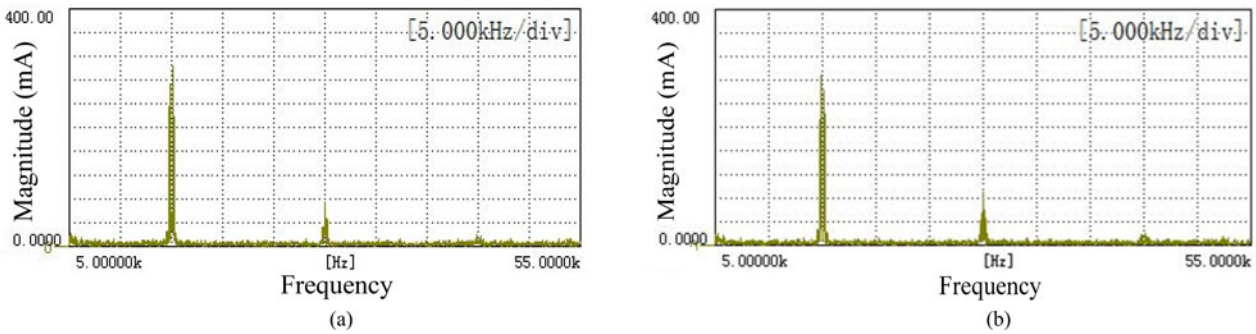


Fig. 15. FFT analysis result of grid current in compared filters. (a) *LCL* filter. (b) Trap filter.

the dominant current harmonics meet the requirement of standard [7], [8] and the filter with the designed parameters can pass the parameter robustness check. And it is also can be found that the worst condition occur while $L_1$, $L_2$, and $L_r$ vary to 95% designed value.

Compared with the traditional parameter robustness analysis method, the proposed method can analyze the conditions of several parameter variations at a time without iteration. In addition, it is very easy to find the weakest performance in all kinds of variation which is useful in parameter optimization.

In additional, it is very important to evaluate the filter performance under weak grid conditions. It is a limit condition for the operation of a grid-connected converter. The weak grid system has a large grid equivalent inductor $L_g$. The grid equivalent inductor $L_g$ can be considered as a part of grid-side inductor $L_2$ and will cause the $L_2$ increase. From Figs. 10(b) and 11(b), it can be found that the increase of $L_2$ will reduce the dominant current harmonics amplitudes. It means the weak grid condition is beneficial for filter performance in the presented filter.

Fig. 12 shows the effect of $L_g$ on the filter resonant frequencies. It can be seen that the $L_g$ has little effect on the second resonant frequency and the frequency of negative resonant peak. This means the weak grid condition will not amplify the switching frequency harmonics due to the variation of the second

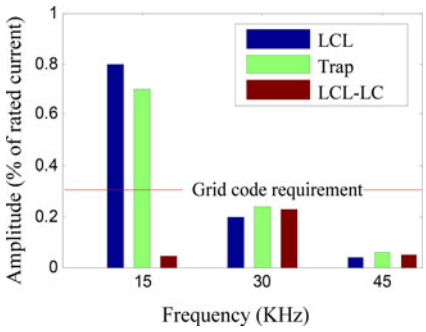


Fig. 16. Current harmonic amplitudes in three filters.

resonant frequency $\omega_2$ and not affect the ability of bypassing switching current harmonics in *LCL-LC* filter. It can also be seen that the increase of $L_g$ will cause the reduction of the first resonant frequency $\omega_1$ which is similar to the traditional *LCL* filter. This means the weak grid condition will reduce the control bandwidth of system and even cause system unstable. It must be carefully considered while designing the controller of converter system.

## VI. Experimental Verification

To verify the aforementioned theoretical analysis, a 5 KW laboratory prototype has been constructed. Three kinds of filters: *LCL* filter, trap filter, and *LCL-LC* filter are used in the prototype, and their performances are compared. The prototype is connected to grid through a step-down transformer with transformation ratio of 380:110. Table IV shows the parameter values of three filters. The converter-side inductor, grid-side inductor, and total capacitor of the three filters are all the same to make sure the costs of different filters are similar. Besides, the components of filters are careful selected to make sure the tolerances of components are less than 5%. A traditional PI controller with grid current feedback is adopted and a 1 Ω resistor is added in the filter capacitor $C$ (or $C_f$) branch to damp system resonance. The performance of different filters are investigated and evaluated under the condition of similar cost.

Fig. 13 shows the measured waveforms of grid current and corresponding fast Fourier transform (FFT) analysis result in presented filter. The maximal current harmonic occurs at the twice switching frequency and its magnitude is 89 mV, which is 0.24% of rated current and is within the range of parameter robustness analysis result in Section V. The experiment results are in good agreement with the theory of parameter robustness analysis. Fig. 14 shows the measured waveform of resonant circuit current and corresponding FFT analysis result in presented *LCL-LC* filter. And it can be found that the major constituent of the resonant circuit current is switching frequency current harmonic. The two currents and their FFT analysis results prove the resonant circuit can bypass the switching frequency harmonics efficiently. Fig. 15 shows the measured grid-side current waveforms and corresponding FFT analysis results of the *LCL* filter and trap filter, respectively. The current harmonic amplitudes caused by PWM in three filters are compared in Fig. 16.

From the experiment results, the following can be seen:

1) The current harmonic amplitude at switching frequency in *LCL-LC* filter is almost equal to zero. It proves that the presented filter has the ability of bypassing switching current harmonics and damping resistor has no effect on this ability.
2) The amplitudes of the twice and triple switching frequency current harmonics in *LCL-LC* filter are lower than the ones of trap filter. It proves that presented filter has a higher rate of high-frequency harmonic attenuation than that of trap filter.
3) The presented filter is the only one which meets the grid code requirement in the three kinds of filters. It validates the performance of designed parameters.
4) The amplitude of switching frequency current harmonic in trap filter is less than the one of *LCL* filter, but still exceeds the requirements of grid code. It proves that the trap filter has the ability of bypassing switching current harmonics but damping resistor will badly weaken its effect.
5) The amplitudes of the twice and triple switching frequency current harmonics in trap filter are greater than the one of *LCL* filter. It proves that the trap filter has the disadvantage of low rate of high-frequency harmonic attenuation.

Experiment results demonstrate the accuracy of theoretical analysis. They prove that the proposed *LCL-LC* filter keeps the advantages of *LCL* and trap filter and overcomes their disadvantages. The results show that the presented filter has the best performance in all three filters and show the effectiveness of the proposed parameter design method and accuracy of the proposed parameter robustness analysis method.

## VII. Conclusion

In this paper, a type filter for grid-connected converter, named *LCL-LC* filter, has been presented. The paper models and analyzes the presented filter. And then two resonant frequency characteristics of the filter are obtained. A parameter design method for the presented filter based on the obtained characteristics is proposed. Then a parameter robustness analysis method is proposed to check the filter performance under the conditions of parameter variations. The following can be concluded:

1) The presented filter has a higher harmonic attenuation rate in the high-frequency band than that of a trap filter and the ability of bypassing switch current harmonics, which is the advantage of a trap filter.
2) The adding of damping resistor has no effect on the bypass ability in presented filter. It means the *LCL-LC* filter overcomes the disadvantage of the trap filter.
3) The proposed parameter design method decomposes the whole filter parameter design into a traditional *LCL* filter part and an *LC* series resonant circuit part. The method can easily make full use of the existing research results about the traditional *LCL* filter parameter design.
4) Compared with the traditional parameter robustness analysis method, the proposed method can check the filter performance under all kinds of parameter variations at a

time and no iteration is needed. Furthermore, it can easily find the weakest condition in all kinds of parameter variations which is very useful in parameter optimization.

5) The theoretical analysis has been fully verified through experiments on a 5 KW prototype. Three kinds of filter—an *LCL* filter, a trap filter, and an *LCL-LC* filter—are compared. The experiment results show that the presented filter has the best performance in all the compared filters.

## REFERENCES


[1] M. Liserre, R. Teodorescu, and F. Blaabjerg, "Stability of photovoltaic and wind turbine grid-connected inverters for a large set of grid impedance values," *IEEE Trans. Power Electron.*, vol. 21, no. 1, pp. 263–272, Jan. 2006.

[2] F. Blaabjerg, R. Teodorescu, M. Liserre, and A. Timbus, "Overview of control and grid synchronization for distributed power generation systems," *IEEE Trans. Ind. Electron.*, vol. 53, no. 5, pp. 1398–1409, Oct. 2006.

[3] R. Teodorescu, M. Liserre, and R. Rodriguez, *Grid Converters for Photovoltaic and Wind Power Systems*. Hoboken, NJ, USA: Wiley, 2011, pp. 2–10.

[4] Y. Tang, P. C. Loh, P. Wang, F. H. Choo, F. Gao, and F. Blaabjerg, "Generalized design of high performance shunt active power filter with output *LCL* filter," *IEEE Trans. Ind. Electron.*, vol. 59, no. 3, pp. 1443–1452, Mar. 2012.

[5] M. Liserre, F. Blaabjerg, and S. Hansen, "Design and control of an *LCL*-filter-based three-phase active rectifier," *IEEE Trans. Ind. Appl.*, vol. 41, no. 5, pp. 1281–1291, Sep./Oct. 2005.

[6] I. J. Gabe, V. F. Montagner, and H. Pinheiro, "Design and implementation of a robust current controller for VSI connected to the grid through an *LCL* filter," *IEEE Trans. Power Electron.*, vol. 24, no. 6, pp. 1444–1452, May/Jun. 2009.

[7] *IEEE Recommended Practices and Requirements for Harmonic Control in Electrical Power Systems*, IEEE Standard 519-1992.

[8] *IEEE Application Guide for IEEE Std. 1547, IEEE Standard for Interconnecting Distributed Resources With Electric Power Systems*, IEEE 1547.2-2008.

[9] W. A. Hill and S. C. Kapoor "Effect of two-level PWM sources on plant power system harmonics," in *Proc. IAS Conf.*, St. Louis, MO, USA, Oct. 1998, pp. 1300–1306.

[10] V. Blasko and V. Kaura, "A novel control to actively damp resonance in input *LC* filter of a three-phase voltage source converter," *IEEE Trans. Ind. Appl.*, vol. 33, no. 2, pp. 542–550, Mar./Apr. 1997.

[11] R. S. Balog and P. T. Krein, "Coupled-inductor filter: A basic filter building block," *IEEE Trans. Power Electron.*, vol. 28, no. 1, pp. 537–546, Jan. 2013.

[12] J. Muhlethaler, M. Schweizer, R. Blattmann, J. W. Kolar, and A. Ecklebe, "Optimal design of *LCL* harmonic filters for three-phase PFC rectifiers," *IEEE Trans. Power Electron.*, vol. 28, no. 7, pp. 3114–3125, Jul. 2013.

[13] Q. Liu, L. Peng, Y. Kang, S. Y. Tang, D. L. Wu, and Y. Qi, "A novel design and optimization method of an *LCL* filter for a shunt active power filter," *IEEE Trans. Ind. Electron.*, vol. 61, no. 8, pp. 4000–4010, Aug. 2014.

[14] H. R. Karshenas and H. Saghafi, "Basic criteria in designing *LCL* filters for grid connected converters," in *Proc. IEEE Int. Symp. Ind. Electron.*, 2006, pp. 1996–2000.

[15] Y. Patel, D. Pixler, and A. Nasiri, "Analysis and design of TRAP and *LCL* filters for active switching converters," in *Proc. IEEE Int. Symp. Ind. Electron.*, 2010, pp. 638–643.

[16] W. M. Wu, Y. B. He, and F. Blaabjerg, "An *LLCL* power filter for single-phase grid-tied inverter," *IEEE Trans. Power Electron.*, vol. 27, no. 2, pp. 782–789, Feb. 2012.

[17] M. Z. Lowenstein and J. F. Hibbard, "Modeling and application of passive-harmonic trap filters for harmonic reduction and power factor improvement," in *Proc. IEEE Ind. Appl. Soc. Annu. Meeting Conf. Rec.*, 1993, pp. 1570–1578.

[18] J. M. Bloemink and T. C. Green, "Reducing passive filter sizes with tuned traps for distribution level power electronics," in *Proc. 14th Eur. Conf. Power Electron. Appl.*, 2011, pp. 1–9.

[19] A. A. Rockhill, M. Liserre, R. Teodorescu, and P. Rodriguez, "Grid-filter design for a multimegawatt medium-voltage voltage-source inverter," *IEEE Trans. Ind. Electron.*, vol. 58, no. 4, pp. 1205–1217, Apr. 2011.

[20] R. Beres, W. Xiongfei, F. Blaabjerg, C. L. Bak, and M. Liserre, "A review of passive filters for grid-connected voltage source converters," in *Proc. Appl. Power Electron. Conf. Expo.*, 2014, pp. 2208–2215.

[21] W. M. Wu, Y. J. Sun, M. Huang, X. F. Wang, H. Wang, F. Blaabjerg, M. Liserre, and H. S. H. Chung, "A robust passive damping method for *LLCL*-filter-based grid-tied inverters to minimize the effect of grid harmonic voltages," *IEEE Trans. Power Electron.*, vol. 29, no. 7, pp. 3279–3289, Jul. 2014.

[22] R. Peña-Alzola, M. Liserre, F. Blaabjerg, R. Sebastián, J. Dannehl, and F. W. Fuchs, "Analysis of the passive damping losses in *LCL*-filter-based grid converters," *IEEE Trans. Power Electron.*, vol. 28, no. 6, pp. 2642–2646, Jun. 2013.

[23] Z. Chi, T. Dragicevic, J. C. Vasquez, and J. M. Guerrero, "Resonance damping techniques for grid-connected voltage source converters with *LCL* filters—A review," in *Proc. IEEE Int. Energy Conf.*, 2014, pp. 169–176.

[24] W. Wu, Y. He, T. Tang, and F. Blaabjerg, "A new design method for the passive damped *LCL* and *LLCL* filter-based single-phase grid-tied inverter," *IEEE Trans. Ind. Electron.*, vol. 60, no. 10, pp. 4339–4350, Oct. 2013.

[25] G. L. Skibinski, "A series resonant sinewave output filter for PWM VSI loads," in *Proc. 37th IAS Annu. Meeting Conf. Rec. Ind. Appl. Conf.*, 2002, vol. 1, pp. 247–256.

[26] J. Xu, J. Yang, J. Ye, Z. Zhang, and A. Shen, "An LTCL filter for three-phase grid-connected converters," *IEEE Trans. Power Electron.*, vol. 29, no. 8, pp. 4322–4338, Aug. 2014.

[27] T. C. Y. Wang, Y. Zhihong, S. Gautam, and Y. Xiaoming, "Output filter design for a grid-interconnected three-phase inverter," in *Proc. IEEE 34th Annu. Power Electron. Spec. Conf.*, 2003, vol. 2, pp. 779–784.

[28] P. Channegowda and V. John, "Filter optimization for grid interactive voltage source inverters," *IEEE Trans. Ind. Electron.*, vol. 57, no. 12, pp. 4106–4114, Dec. 2010.

[29] Z. Xing, Z. Hong, L. Fei, L. Fang, L. Chun, and L. Benxuan, "An *LCL-LC* power filter for grid-tied inverter," in *Proc. TENCON IEEE Region 10 Conf. (31194)*, 2013, pp. 1–4.

[30] M. Liserre, F. Blaabjerg, and A. Dell'Aquila, "Step-by-step design procedure for a grid-connected three-phase PWM voltage source converter," *Int. J. Electron.*, vol. 91, pp. 445–460, 2004.

[31] C. Bao, X. Ruan, X. Wang, W. Li, D. Pan, and K. Weng, "Step-by-step controller design for *LCL*-type grid-connected inverter with capacitor–current-feedback active-damping," *IEEE Trans. Power Electron.*, vol. 29, no. 3, pp. 1239–1253, Mar. 2014.

[32] M. Y. Park, M. H. Chi, J. H. Park, H. G. Kim, T. W. Chun, and E. C. Nho, "*LCL*-filter design for grid-connected PCS using total harmonic distortion and ripple attenuation factor," in *Proc. Int. Power Electron. Conf.*, 2010, pp. 1688–1694.

[33] D. Ricchiuto, M. Liserre, T. Kerekes, R. Teodorescu, and F. Blaabjerg, "Robustness analysis of active damping methods for an inverter connected to the grid with an *LCL*-filter," in *Proc. IEEE Energy Convers. Congr. Expo.*, 2011, pp. 2028–2035.

[34] Y. A. R. I. Mohamed, M. A. Rahman, and R. Seethapathy, "Robust line-voltage sensorless control and synchronization of *LCL*-filtered distributed generation inverters for high power quality grid connection," *IEEE Trans. Power Electron.*, vol. 27, no. 1, pp. 87–98, Jan. 2012.

[35] D. G. Holmes and T. A. Lipo, *Pulsewidth Modulation for Power Converters: Principles and Practice.* Hoboken, NJ, USA: Wiley, 2003, pp. 215–336.


**Fei Li** (S'13) was born in Anhui, China, in 1984. He received the B.S. degrees in electric engineering and automation in 2008 from Hefei University of Technology, Hefei, China, where he is currently working toward the Ph.D. degree in electric engineering and automation.

His current research interests include filter topology and parameter design, harmonic mitigation in parallel converter systems, and photovoltaic generation technologies.

**Xing Zhang** (M'13–SM'14) was born in Shanghai, China, in 1963. He received the B.S., M.S., and Ph.D. degrees in electric engineering and automation from Hefei University of Technology, Hefei, China, in1984, 1990, and 2003, respectively.

Since 1984, he has been a Faculty Member of the School of Electric Engineering and Automation, Hefei University of Technology, where he is currently a Professor and is also at the Photovoltaic Engineering Research Center of Ministry of Education. His current research interests include photovoltaic generation technologies, wind power generation technologies, and distributed generation system.

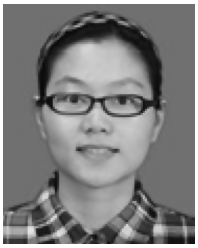

**Hong Zhu** was born in Anhui, China, in 1989. She received the B.S. degree in electric engineering and automation in 2012 from Hefei University of Technology, Hefei, China, where she is currently working toward the Ph.D. degree in electric engineering and automation.

Her current research interests include filter design, grid simulator design, and photovoltaic generation technologies.

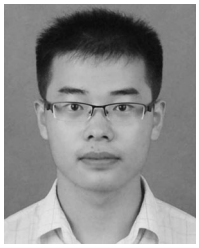

**Haoyuan Li** was born in Henan, China, in 1990. He received the B.S. degree in electric engineering and automation in 2013 from Hefei University of Technology, Hefei, China, where he is currently working toward the Ph.D. degree in electric engineering and automation.

His current research interests include electric vehicle technologies and parameters design for power electronic systems.

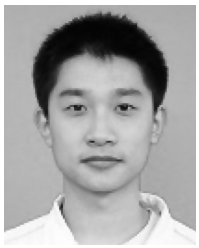

**Changzhou Yu** (S'13) was born in Sichuan, China, in 1987. He received the B.S. degree in electric engineering and automation in 2009 from Hefei University of Technology, Hefei, China, where he is currently working toward the Ph.D. degree in electric engineering and automation.

His current research interests include control of PWM converters, parallel converter systems, and photovoltaic generation technologies.